

Conical Intersections in Laboratory Coordinates with Ultracold Molecules

Alisdair O. G. Wallis,¹ S. A. Gardiner,² and Jeremy M. Hutson¹

¹*Department of Chemistry, Durham University, South Road, Durham, DH1 3LE, United Kingdom*

²*Department of Physics, Durham University, South Road, Durham, DH1 3LE, United Kingdom*

(Received 11 May 2009; published 17 August 2009)

For two states of opposite parity that cross as a function of an external magnetic field, the addition of an electric field will break the symmetry and induce an avoided crossing. A suitable arrangement of fields may be used to create a conical intersection as a function of external spatial coordinates. We consider the effect of the resulting geometric phase for ultracold polar molecules. For a Bose-Einstein condensate in the mean-field approximation, the geometric phase effect induces stable states of persistent superfluid flow that are characterized by half-integer quantized angular momentum.

DOI: 10.1103/PhysRevLett.103.083201

PACS numbers: 34.50.-s, 03.65.Nk, 34.10.+x, 82.20.Xr

It is well known that the potential energy surfaces for molecular electronic states of the same symmetry can cross at a point in two dimensions or on a surface of dimension $n - 1$ in n dimensions. These crossings are known as conical intersections because the two surfaces locally form a double cone. Conical intersections have a wealth of interesting consequences for molecular structure and dynamics. For example, they are responsible for the Jahn-Teller effect [1] and play an important role in non-adiabatic processes [2]. One of the most interesting consequences of conical intersections is the *geometric phase* (Berry phase) effect [3]: when the nuclei follow a path that encircles a conical intersection once and returns to the original configuration (pseudorotation), the electronic wave function changes sign. Since the *total* wave function must be a single-valued function of coordinates, this requires that the wave function for nuclear motion must also change sign. This has important dynamical consequences: it produces half-odd-integer quantization for free pseudorotation [4] and may have significant effects on collision cross sections [5].

The purpose of this Letter is to explore conical intersections of a different type. It is now possible to produce atomic and molecular Bose-Einstein condensates (BECs) and to subject them to applied magnetic and electric fields. The atomic and molecular states split and shift as a function of the magnetic field (Zeeman effect) and electric field (Stark effect). In the absence of an electric field, parity is conserved, so it is possible to tune the magnetic field so that two levels of different parity are exactly degenerate with one another. However, if a simultaneous electric field is applied, the two levels of opposite parity are mixed and the degeneracy is resolved [6]. Conical intersections can thus occur at points where the electric field is zero. It is possible to envisage an arrangement of fields that creates conical intersections between two atomic or molecular levels as a function of external spatial coordinates rather than internal coordinates.

All the results that apply to conical intersections between molecular potential energy surfaces will continue to apply in this new situation. The internal (electronic, vibrational, or spin) wave function of the atom or molecule will change sign along a path that encircles the intersection once, so the spatial wave function of the condensate must also change sign.

Quantized vortices are a characteristic sign of superfluid flow [7], and since their first observation in the context of Bose-Einstein condensed dilute atomic gases [8] they have been key to some spectacular experimental results [9,10]. Recent experiments placing a BEC within a toroidal trapping geometry [11–13] have enabled the observation of persistent flow around a toroidal trap [11]. The possibility of forming half-integer quantized vortices within a spinor atomic BEC configuration has been investigated theoretically [14–17], as have a variety of differing consequences of geometric phase effects in atomic BEC systems [18–21]. In this work we combine these different threads to show how, with an appropriate configuration of magnetic and electric fields, a BEC of heteronuclear diatomic molecules will assume a toroidal geometry, such that the geometric phase causes the system to manifest macroscopically occupied states of half-integer quantized persistent flow.

Effects of this type can in principle be observed in any system where two states of opposite parity can be tuned into degeneracy with a magnetic field and can be coupled with an electric field. However, for atomic systems states of different parity are usually far apart at zero field. More accessible examples are provided by gases of heteronuclear alkali-metal dimers such as RbCs and KRb, which are the targets of current experiments. In the present work we illustrate the effect for a gas of KRb molecules in a single vibrational level of the lowest triplet state, $^3\Sigma^+$.

The energy levels of a $^3\Sigma^+$ molecule in an applied field are conveniently expanded in a fully decoupled basis set of functions $|NM_N\rangle|SM_S\rangle$, where N and S are quantum numbers for molecular rotation and electron spin and M_N and

M_S are the corresponding space-fixed projections onto the magnetic field axis. Nuclear spin is neglected here for simplicity. A simple form of the Hamiltonian that contains all the essential ingredients is

$$H = B\hat{N}^2 + \frac{2}{3}\lambda(\hat{S}^2 - 3\hat{S}_Z^2) + g_e\mu_B B_Z M_S - \boldsymbol{\mu} \cdot \mathbf{E}, \quad (1)$$

where B is the molecular rotational constant, λ is the spin-spin coupling constant, S_Z is the projection of S onto the molecular axis, B_Z is the magnetic field orientated along the space-fixed Z axis, and \mathbf{E} and $\boldsymbol{\mu}$ are the vectors representing the electric field and molecular electric dipole moment. KRb has not been characterized in detail spectroscopically, but ultracold KRb has recently been formed in the lowest rovibrational levels of both singlet and triplet states [22]. Electronic structure calculations give an equilibrium distance $r_e = 5.901 \text{ \AA}$ for the triplet state [23]. This allows B and λ for the lowest vibrational level to be estimated as $B = 0.01813 \text{ cm}^{-1}$ and $\lambda = -0.00632 \text{ cm}^{-1}$. The dipole moment function has been

calculated by Kotochigova, Tiesinga, and Julienne [24] and has a value around 0.051 D near r_e .

Figure 1 shows the lowest rotational levels of KRb ($a^3\Sigma^+$) as a function of magnetic field in the presence and absence of a moderate electric field (5 kV/cm). At zero field, the $N = 0$ level has a single sublevel with total angular momentum $J = 1$, while the $N = 1$ level is split into 3 sublevels with $J = 0, 1$, and 2 . When a magnetic field is applied, each sublevel is split into $2J + 1$ components labeled by M_J . At zero electric field, the $M_J = +1$ level originating from $N = 0, J = 1$ and the $M_J = 0$ level originating from $N = 1, J = 1$ have different parity and cross near $B_Z = 187 \text{ G}$.

When a nonzero electric field is introduced, parity is no longer conserved. However, if the electric and magnetic fields are parallel, M_J is conserved and $M_J = 0$ and $+1$ states cross. We have therefore chosen the electric field to be perpendicular to the magnetic field to induce an avoided crossing between the $M_J = 0$ and $+1$ states as shown in Fig. 1.

We may envisage an experiment in which a BEC is subjected to a magnetic field B_Z , orientated along the space-fixed Z axis, which varies along the X axis with field gradient dB_Z/dX . An inhomogeneous electric field \mathbf{E} is oriented along the X axis with a magnitude which varies with Y as dE/dY , vanishing on a plane at $Y = 0$. This creates a seam of conical intersections along the line $0, 0, Z$ where $X = 0$ is the position at which the magnetic field brings the two states into degeneracy. Adding an external cylindrically symmetric optical trapping potential in the XY plane of the electromagnetic field gradients, $V_{\text{opt}}(\rho, \phi, Z) = \frac{1}{2}M(\omega_\rho^2\rho^2 + \omega_Z^2Z^2)$, where $\rho^2 = X^2 + Y^2$, creates a toroidally shaped potential around the conical intersection, with a radial minimum at ρ_0 . The left-hand side of Fig. 2 shows the resulting potential for a magnetic field gradient of 5 G/cm , an electric field gradient of 6.8 kV/cm^2 , and an optical trapping potential with a height of 7 \mu K at $\rho = 30 \text{ \mu m}$ [25] centered at the conical intersection. This potential has significant anisotropy (about 10 nK), which is manifested as an asymmetry along a cut with $Y = 0$ as shown schematically in the lower panel.

The anisotropy of the toroidal trapping potential $V_{\text{trap}}(\phi)$ can be controlled by offsetting the optical trapping potential from the point of intersection. Assuming that the Zeeman effect is linear over the range of the intersection, with respective gradients a and b , the asymmetry along $Y = 0$ will be zero when the optical trap is centered at $x_0 = (a + b)/(2M\omega_\rho)$. The trapping potential still has slightly different depths along the X and Y axes, but this can be minimized by adjusting the electric field gradient. The right-hand side of Fig. 2 shows the resulting optimized trapping potential, with $x_0 = 0.0715 \text{ \mu m}$ and $dE/dY = 6.723 \text{ kV/cm}^2$. This potential has an angular anisotropy on the order of 0.01 nK .

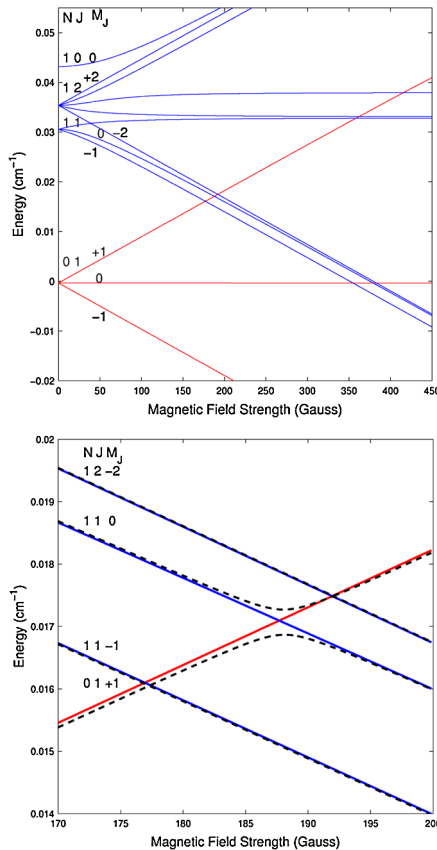


FIG. 1 (color online). Energy levels of KRb as a function of magnetic field B . The upper panel shows an overview, with each zero-field level [labeled by (N, J)] splitting into $2J + 1$ components as a function of magnetic field. The lower panel shows how two levels of different parity cross ($M_J = 0$ and $+1$) in the absence of an electric field (solid lines) but avoid one another in the presence of a 5 kV/cm electric field (dashed lines).

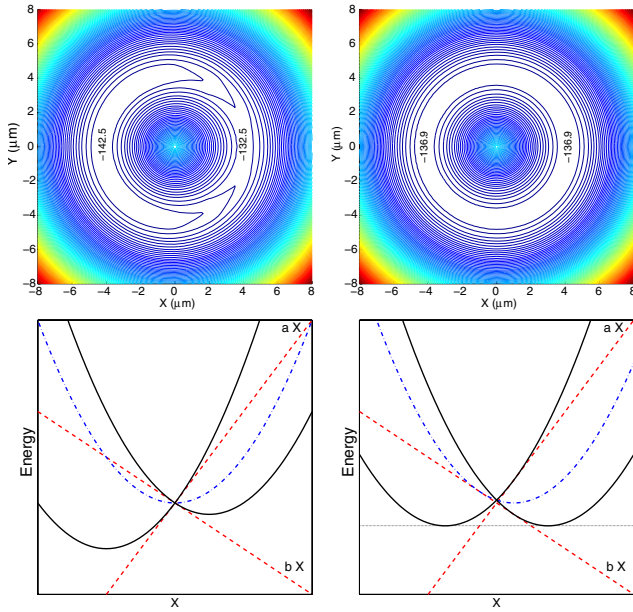


FIG. 2 (color online). Toroidal potentials formed around conical intersections. Left-hand panels: Potential formed when the optical trapping potential (7 nK at $30 \mu\text{m}$) is centered at the point of intersection ($\rho = 0$), with field gradients $5 \text{ G/cm } \hat{\mathbf{X}}$ and $6.8 \text{ kV/cm}^2 \hat{\mathbf{Y}}$. Right-hand panels: Potential formed when the trapping potential is offset along $\hat{\mathbf{X}}$ by $x_0 = 0.0715 \mu\text{m}$, with field gradients $5 \text{ G/cm } \hat{\mathbf{X}}$ and $6.723 \text{ kV/cm}^2 \hat{\mathbf{Y}}$. The electric field gradient is chosen to minimize the anisotropy in each case. The well depths are given in nK relative to the point of intersection. The lower panels show schematic cuts through the potential at $Y = 0$: KRB eigenstates (red dashed lines), optical trapping potential (blue dot-dashed lines), and the resultant toroidal potential (black solid lines).

For a molecule of mass M moving in a toroidal potential such as those in Fig. 2, the single-particle Schrödinger equation is approximately separable, with solutions $\Psi(\rho, \phi, Z) = \psi(\rho)\Phi(\phi)\varphi(Z)$. In the absence of anisotropy, the geometric-phase-induced antiperiodic boundary condition $\Phi(\phi) = -\Phi(\phi + 2\pi)$ gives $\Phi(\phi) = (2\pi)^{-1/2} \exp(im\phi)$, where m takes half-integer values $\pm\frac{1}{2}, \pm\frac{3}{2}, \pm\frac{5}{2}$, etc. If the boundary conditions were periodic over 2π , m would take integer values $0, \pm 1, \pm 2$, etc. For periodic boundary conditions the ground state has zero angular momentum $m = 0$, but for antiperiodic boundary conditions it has a nonzero angular momentum $m = \pm\frac{1}{2}$. The single-particle energy spectrum is

$$E = \left(\nu_z + \frac{1}{2}\right)\hbar\omega_z + \left(\nu_\rho + \frac{1}{2}\right)\hbar\omega_\rho + b_{\text{rot}}\left(m^2 - \frac{1}{4}\right), \quad (2)$$

where the third term represents the rotational energy of the particle with a rotational constant $b_{\text{rot}} = \hbar^2/2M\rho_0^2$.

In order for geometric phase effects to be observed, the angular anisotropy of the toroidal trapping potential $V_{\text{trap}}(\phi)$ must be small enough to allow the wave function to fully encircle the intersection. For the potentials shown

in Fig. 2, $\frac{1}{2}\hbar\omega_\rho \approx 4 \text{ nK}$ and $b_{\text{rot}} \approx 0.5 \text{ nK}$. For the potential on the left-hand side, the anisotropy is large compared to b_{rot} , so that the single-particle wave function will be localized on one side of the trap. However, for the potential on the right-hand side, the anisotropy is small compared to b_{rot} and the single-particle wave function will fully encircle the conical intersection and exhibit half-integer quantization.

A BEC of a dilute gas may be modeled by the Gross-Pitaevskii equation (GPE). The time-independent GPE is

$$[\hat{H}_0 + u(\phi)|\Psi(\rho, \phi, Z)|^2]\Psi(\rho, \phi, Z) = \mu\Psi(\rho, \phi, Z), \quad (3)$$

where μ is the chemical potential and the mean-field wave function Ψ is normalized to unity, $\int \Psi^*\Psi d\tau = 1$. The effective interaction strength $u(\phi)$ is $4\pi\hbar^2 Na(\phi)/M$, where N is the number of particles in the condensate. The internal molecular wave function at angle ϕ may be written in terms of the individual molecular states ψ_1 and ψ_2 as

$$\psi(\phi) = \psi_1 \cos(\phi/2) + \psi_2 \sin(\phi/2), \quad (4)$$

so the effective angle-dependent scattering length $a(\phi)$ is

$$a(\phi) = \frac{1}{8}(3a_{11} + 3a_{22} + 2a_{12}) + \frac{1}{2}(a_{11} - a_{22}) \times \cos\phi + \frac{1}{8}(a_{11} + a_{22} - 2a_{12})\cos 2\phi, \quad (5)$$

where a_{ij} is the scattering length for interaction between molecules in states i and j . This is isotropic in the case $a_{11} = a_{22} = a_{12}$.

Averaging over the radial and vertical wave functions gives an effective 1D GPE in ϕ ,

$$\left[-b_{\text{rot}}\frac{\partial^2}{\partial\phi^2} + \tilde{u}(\phi)|\Phi(\phi)|^2\right]\Phi(\phi) = \tilde{\mu}\Phi(\phi), \quad (6)$$

where

$$\tilde{u}(\phi) = \frac{4\pi\hbar^2 Na(\phi)}{M} \iint |\psi(\rho)|^4 |\varphi(Z)|^4 \rho d\rho dZ \quad (7)$$

and $\mu = \tilde{\mu} + (\nu_z + \frac{1}{2})\hbar\omega_z + (\nu_\rho + \frac{1}{2})\hbar\omega_\rho - b_{\text{rot}}/4$. For a flat ring, this has analytical solutions $\Phi(\phi) = (2\pi)^{-1/2} \exp(im\phi)$, with $\tilde{\mu} = b_{\text{rot}}m^2 + \tilde{u}/(2\pi)$. Applying antiperiodic boundary conditions, we obtain the same solutions as for the single-particle case, namely, states of half-integer quantized angular momentum.

In the presence of a small anisotropy, there are two classes of solution satisfying antiperiodic boundary conditions: flowing solutions, $\Phi_m^\pm(\phi) \approx (2\pi)^{-1/2} \times \exp(\pm im\phi)$, and static solutions, such as $\Phi_m^0(\phi) \approx \pi^{-1/2} \cos(m\phi)$ for small interactions, both with half-integer m . For a trap with a residual anisotropy $V_{\text{trap}}(\phi) = -V_1 \cos\phi - V_2 \cos 2\phi$ and an angle-dependent interaction strength $\tilde{u}(\phi) = u_0 + u_1 \cos\phi + u_2 \cos 2\phi$, we obtain ap-

proximate chemical potentials corresponding to these two Ansätze of $\tilde{\mu}_{1/2}^{\pm} \approx b_{\text{rot}}/4 + u_0/(2\pi)$ and $\tilde{\mu}_{1/2}^0 \approx b_{\text{rot}}/4 - V_1/2 + 3u_0/(4\pi) - u_1/(2\pi) - u_2/(8\pi)$. In this approximation, a flowing state with $m = \pm 1/2$ is the ground state if $2u_1 + u_2/2 + 2\pi V_1 < u_0$. For any given $a(\phi)$ and condensate number, we can apply an offset of the optical potential sufficient to compensate for the anisotropy of the interaction term and stabilize the flowing state.

The permitted velocities of the persistent flow can assume only half-integer values compared to the quantized units of circulation possible in a more conventional single-species atomic BEC in a comparable toroidal geometry [11]. The persistent flow should be observable by releasing the trapped particles and employing a time-of-flight technique [11].

A BEC such as described here is stable only if $a(\phi)$ remains positive all around the ring. From Eq. (5), this requires that a_{11} and a_{22} are both positive and that $2a_{12} > -(a_{11} + a_{22})$. In addition, a condensate of polar molecules can undergo dipolar collapse [26] if the dipole length a_d exceeds the scattering length for the short-range interactions, where $a_d = |d^2|M/(12\pi\epsilon_0\hbar^2)$ and d is the effective dipole moment of the molecule in the field. Since the molecular wave function is given by Eq. (4) and there is a direct dipole moment matrix element $\langle 1|\mu|2\rangle$ between the near-degenerate states ψ_1 and ψ_2 , $d = \langle 1|\mu|2\rangle \sin\phi$. For the two states of KRB considered here, $\langle 1|\mu|2\rangle \sim 10^{-32}$ C m, which gives $a_d^{\text{max}} \sim 5 \times 10^{-12}$ m. This is substantially smaller than typical scattering lengths so dipolar collapse is unlikely.

The present Letter has described a novel form of conical intersection that can occur as a function of three-dimensional laboratory coordinates, instead of internal molecular coordinates. Using such conical intersections, it may be possible to create novel superfluid states with stable persistent flow characterized by half-integer, rather than integer quantized angular momentum. Although we have considered the effect for polar molecules, a similar effect might be produced for well-separated levels, perhaps even in atoms, using a laser field to bring the levels into near-degeneracy and an inhomogeneous magnetic field to provide a crossing. Conical intersections would appear at points of zero laser amplitude, for example, at the nodes in an optical lattice.

The effect proposed here can in principle be observed in any system where two states of any different symmetry (not just parity) can be tuned into degeneracy with one external influence, and then split apart again with another influence that breaks the symmetry.

The authors are grateful to EPSRC and for funding the collaborative project QuDipMol under the ESF EUROCORES program EuroQUAM.

- [1] H. C. Longuet-Higgins, U. Opik, M. H. L. Pryce, and R. A. Sack, Proc. R. Soc. A **244**, 1 (1958).
- [2] *Conical Intersections: Electronic Structure, Dynamics and Spectroscopy*, edited by W. Domcke, D. R. Yarkony, and H. Köppel (World Scientific, Singapore, 2004).
- [3] M. V. Berry, Proc. R. Soc. A **392**, 45 (1984).
- [4] H. von Busch, V. Dev, H.-A. Eckel, S. Kasahara, J. Wang, W. Demtröder, P. Sebald, and W. Meyer, Phys. Rev. Lett. **81**, 4584 (1998).
- [5] J. C. Juanes-Marcos and S. C. Althorpe, J. Chem. Phys. **122**, 204324 (2005).
- [6] B. Friedrich and D. Herschbach, Phys. Chem. Chem. Phys. **2**, 419 (2000).
- [7] J. Annett, *Superconductivity, Superfluids, and Condensates* (Oxford University Press, Oxford, 2004).
- [8] M. R. Matthews, B. P. Anderson, P. C. Haljan, D. S. Hall, C. E. Wieman, and E. A. Cornell, Phys. Rev. Lett. **83**, 2498 (1999).
- [9] C. Raman, J. R. Abo-Shaer, J. M. Vogels, K. Xu, and W. Ketterle, Phys. Rev. Lett. **87**, 210402 (2001).
- [10] A. E. Leanhardt, A. Görlitz, A. P. Chikkatur, D. Kielpinski, Y. Shin, D. E. Pritchard, and W. Ketterle, Phys. Rev. Lett. **89**, 190403 (2002).
- [11] C. Ryu, M. F. Andersen, P. Clade, V. Natarajan, K. Helmerson, and W. D. Phillips, Phys. Rev. Lett. **99**, 260401 (2007).
- [12] A. S. Arnold, C. S. Garvie, and E. Riis, Phys. Rev. A **73**, 041606(R) (2006).
- [13] K. Henderson, C. Ryu, C. MacCormick, and M. G. Boshier, New J. Phys. **11**, 043030 (2009).
- [14] F. Zhou, Phys. Rev. Lett. **87**, 080401 (2001).
- [15] J. Ruostekoski and J. R. Anglin, Phys. Rev. Lett. **91**, 190402 (2003).
- [16] H. Chiba and H. Saito, Phys. Rev. A **78**, 043602 (2008).
- [17] S. Hoshi and H. Saito, Phys. Rev. A **78**, 053618 (2008).
- [18] I. Fuentes-Guridi, J. Pachos, S. Bose, V. Vedral, and S. Choi, Phys. Rev. A **66**, 022102 (2002).
- [19] Z.-D. Chen, J.-Q. Liang, S.-Q. Shen, and W.-F. Xie, Phys. Rev. A **69**, 023611 (2004).
- [20] C. Zhang, A. M. Dudarev, and Q. Niu, Phys. Rev. Lett. **97**, 040401 (2006).
- [21] V. M. Kaurov and A. B. Kuklov, Phys. Rev. A **73**, 013627 (2006).
- [22] K.-K. Ni, S. Ospelkaus, M. H. G. de Miranda, A. Pe'er, B. Neyenhuis, J. J. Zirbel, S. Kotochigova, P. S. Julienne, D. S. Jin, and J. Ye, Science **322**, 231 (2008).
- [23] S. Rousseau, A. R. Allouche, and M. Aubert-Frécon, J. Mol. Spectrosc. **203**, 235 (2000).
- [24] S. Kotochigova, E. Tiesinga, and P. S. Julienne, Eur. Phys. J. D **31**, 189 (2004).
- [25] T. Takekoshi, B. M. Patterson, and R. J. Knize, Phys. Rev. Lett. **81**, 5105 (1998).
- [26] T. Koch, T. Lahaye, J. Metz, B. Fröhlich, A. Griesmaier, and T. Pfau, Nature Phys. **4**, 218 (2008).